Mechanisms of CH_4, H_2S and SO_2 Oxidation on Precious Metal Catalysts under stagnation point flow conditions

G. Rickett[1], V. Dupont[1*], and M. V. Twigg[2]

[1]Energy Resource Institute, SPEME, The University of Leeds, Leeds, LS2 9JT, UK
[2]Jonhson Matthey, Catalytic Systems Division, Orchard Road, Royston, SG8 5HE, UK

Corresponding author: V.Dupont@leeds.ac.uk

Paper accepted and published. Full reference:
Rickett, G., Dupont, V., Twigg, M.V., 2006. Kinetics of CH_4, H_2S and SO_2 oxidation on precious metal catalysts under stagnation point flow conditions. Journal of the Energy Institute, Vol. 79, No.1 pp.12-18.

ABSTRACT

A new methodology which combines reactor experiments and numerical modelling to derive kinetic rates of solid-gas heterogeneous reactions in a stagnation point flow reactor (SPFR) is developed and used to investigate the effects of small concentrations of H_2S and SO_2 on the lean catalytic combustion of methane on precious metal catalysts. The activity of polycrystalline Pt foil, then Pt, Rh and Pd- containing washcoats supported on stainless steel foils are investigated in the SPFR, where the washcoat consisted of a thin layer of γ-Alumina or ceria/γ-alumina. The porous washcoats supported on steel foil were more active than the equivalent flat surface of pure precious metal (case of Pt) with pre-exponential factors of 7.4×10^5 cm s^{-1} and 4.9×10^4 cm s^{-1} respectively. Repeated use of the washcoated catalyst add the effect of pore opening given rise to a change in the pre-exponential factor from 7.4×10^5 cm s^{-1} to 1.1×10^9 cm s^{-1} for Pt. The high temperature activity behaviour of Pt in presence of sulphur species in the feed was however superior to that of Pd, due to the changing nature of the active site in CH_4 oxidation (PdO/Pd), as is consistent with the literature based on other type of reactor studies. Methane combustion was enhanced by both H_2S and SO_2 on the Pt catalysts as opposed to the Pd and Rh catalysts, which saw a decrease in the methane conversion.

Keywords: kinetic, catalytic, modelling, methane, and sulphur

1 Introduction

The benefits of catalytic combustion over conventional gas phase combustion are near zero NO_X, CO and unburned hydrocarbon emissions when operating in the ultra fuel-lean regime, due to the low temperatures and complete heterogeneous oxidation. Catalytic reactions can also add stability to the combustion process in certain conditions, increasing its safety by reducing risks of explosion or flame extinction. With the diversification of fuel sources from the processing of low-CV biomass or waste fuels, hydrocarbon gas mixtures containing traces of sulphur species are becoming the focus of increasing research as potential fuels for catalytic combustion processes. Whereas the poisoning effects of sulphur-species in 3-way catalytic converters are now well known, there is comparatively less data in catalytic burners. Most studies to date involve experiments in isothermal plug-flow or well-stirred micro-reactors [1-3], which indicate that all precious metal catalysts are poisoned to a certain extent by the presence of the S-species. Their ability to regenerate under certain conditions then varies, among other parameters, on the nature of the precious metal.

By contrast, the stagnation point flow reactor (SPFR) offers a reacting boundary layer configuration that is closer to many real catalytic combustion devices, such as the channels of honeycomb catalytic monoliths, or other coated surfaces used for heat transfer as the seat of the catalytic oxidation reactions. To date, SPFR studies have rarely been directly at the source of systematically derived kinetic data, to the exception of Perger *et al*'s recent work on ignition kinetics [4], being used instead to validate proposed mechanisms [5]. In the present work, we employ a new methodology permitting the derivation of kinetic rates of catalytic oxidation reactions in the SPFR [6], and contrast its results with those obtained in isothermal plug flow conditions with the same (or similar) catalytic material and reactant mixtures.

2 Experimental

Figure 1 shows a diagram of the experimental SPFR. The mass flow rate of CH_4, N_2 and air where regulated by three mass flow controllers. The gas mixture flows of $CH_4/O_2/N_2$ are defined by the air to fuel ratio with values between 11 and 43 (by volume), i.e. fuel-lean (stoichiomentric 9.5). The concentrations of CH_4 and O_2 at the injector were changed between 3.6 %vol and 1.2 %vol for methane and 8.4 %vol and 10.8 %vol for air. The concentration of N_2 was kept constant at 88 %vol by additional N_2.

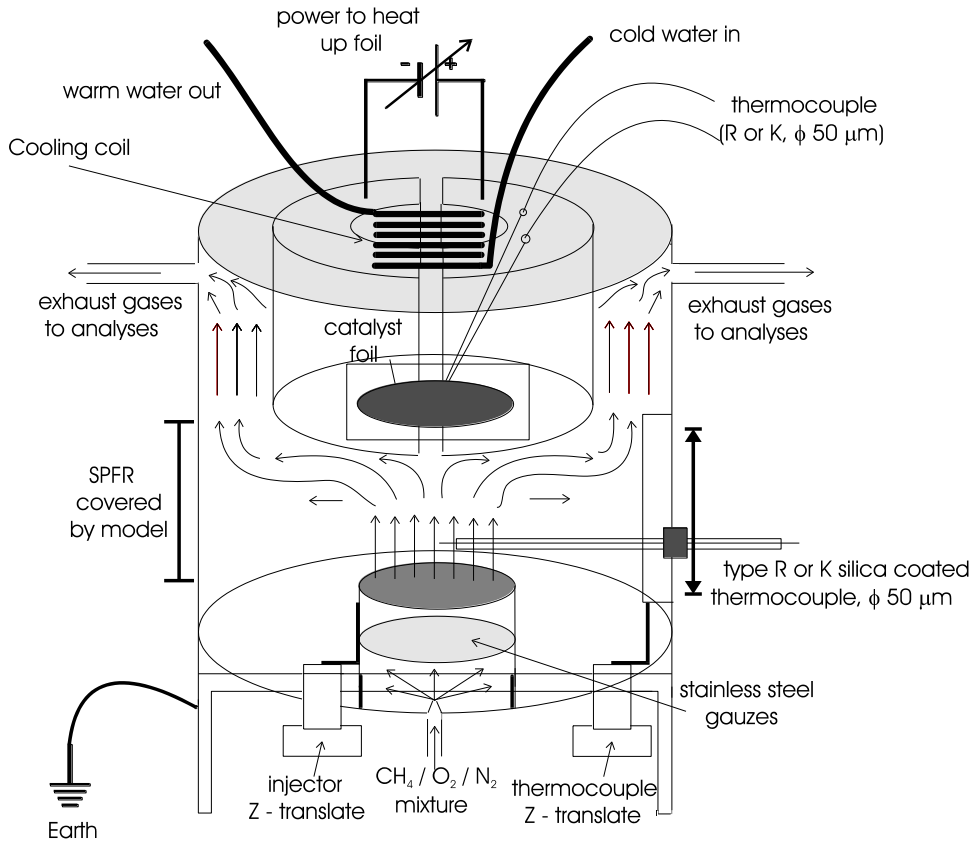

Fig. 1 Diagram of the SPFR.

The gas mixture flowed perpendicularly onto the electrically heated foils of controlled set-temperature from a distance of 3 mm with velocities ranging between 1.7 and 3.4 cm s^{-1} (STP). Concentrations between 30 and 100 ppm of H_2S or SO_2 were utilised by means of a programmable syringe pump when studying the effects of S-species in the gas feed.

The catalyst foils were polycrystalline Pt foil 100 μm thick, and stainless steel foils, the latter covered with washcoats of γ-Al_2O_3 and 12% wt. CeO_2/γ-Al_2O_3 5-10 μm thick (determined by SEM) and containing either 3.79 %wt. Pt, 2.07 %wt. Pd or 2%wt. Rh, corresponding to the same molar concentrations. In their yet unused and calcined state (450 °C in a flow of air), the Al_2O_3 and CeO_2/Al_2O_3 washcoats were characterized by BET surface areas of 157.3 and 131.9 m^2/g, and average pore diameters of 4.7 and 4.5 nm respectively (based on the adsorption branch due to consideration of pore-shape). Precious metal particle sizes were in the 1-2 nm range (TEM) prior to use of the catalysts.

The exhaust gases were analysed using two on-line analysers, an SO_2 UV absorption analyser on a wet basis (± 1ppm) and an O_2 paramagnetic analyser on a dry basis (± 500ppm). It was shown

that no CO was produced and the rate of reaction of CH_4 oxidation was calculated by means of an O_2 balance.

The reactor was designed to approach the theoretical model of the stagnation point flow as much as possible. A low ratio (0.128) of separation distance of injector-foil to foil diameter was used to simulate the ideal geometry, which assumes infinite diameters of injector and catalyst, and allows the assumption of lack of temperature and concentration gradients in the radial direction. Modelling of the SPFR in the domain delimited by the region between the injector and the foil is then simplified to the solution of the conservation equations with a pseudo-one-dimensional treatment.

3 Modelling

The code SPIN [7] and a post-processing code written by the authors [8] were used to model the evolution of the conversion of the CH_4 and S-species reactants with the catalyst temperature (T_S). In the absence of gas phase reactions, the conversion is the ratio of the net molar flux of the reactant at the catalyst surface (predicted by the code, and itself proportional to the heterogeneous reaction rate) to its molar influx at the injector, a known boundary condition. Thus, given an Arrhenius description of the heterogeneous reaction rate of this reactant at the catalyst ($k = A\times\exp(-E/RT_S)$), one can relate a function of the conversion (cv_R) and T_S to the unknown values A and E as described in Eq. 1.

$$\ln\left(\left(\frac{P}{R}\right)^{-(a+b)} \times T_S{}^{(a+b)} \times \frac{K_1 cv_R}{\left(K_2 + K_3 cv_R\right)^a \left(K_4 + K_5 cv_R\right)^b}\right) = \ln A - \frac{E}{RT_S} \quad (Eq.1)$$

Where P is the total pressure, R is the universal gas constant, a and b are the chosen reactant orders of CH_4 (or S-species) and O_2, which are ideally predetermined by appropriate experiments (i.e. initial rate method). Here, the initial rate method confirmed order 0 for O_2 and 1 for CH_4 and SO_2. The constants K_2-K_5, where $X_{CH4,S\ or\ SO2,S} = K_2 + K_3\, cv_R$ and $X_{O2,S} = K_4 + K_5\, cv_R$, and $X_{i,S}$ is the mol fraction of species i at the gas-catalyst's interface can be determined easily by running the code SPIN twice with assumed values of A and E, from which they have been found to be independent. For a more detailed explanation of this equation, we refer the reader to [6]. A linear regression performed on the *LHS* of Eq. 1 and T_S^{-1} then yields best the fit values of A and E.

4 Results and Discussion

4.1 Kinetics of CH_4 oxidation on Pt catalysts

Figure 2 shows the linear fits of the *LHS* of Eq. 1 for CH_4 oxidation in the presence and absence of a sulphur species when using Pt catalysts at various stages in their lifetime and use. The experimental points shown in Fig. 2 and used in the fitting are only those for which the conversion was controlled by chemical kinetics, i.e. typically below 50%.

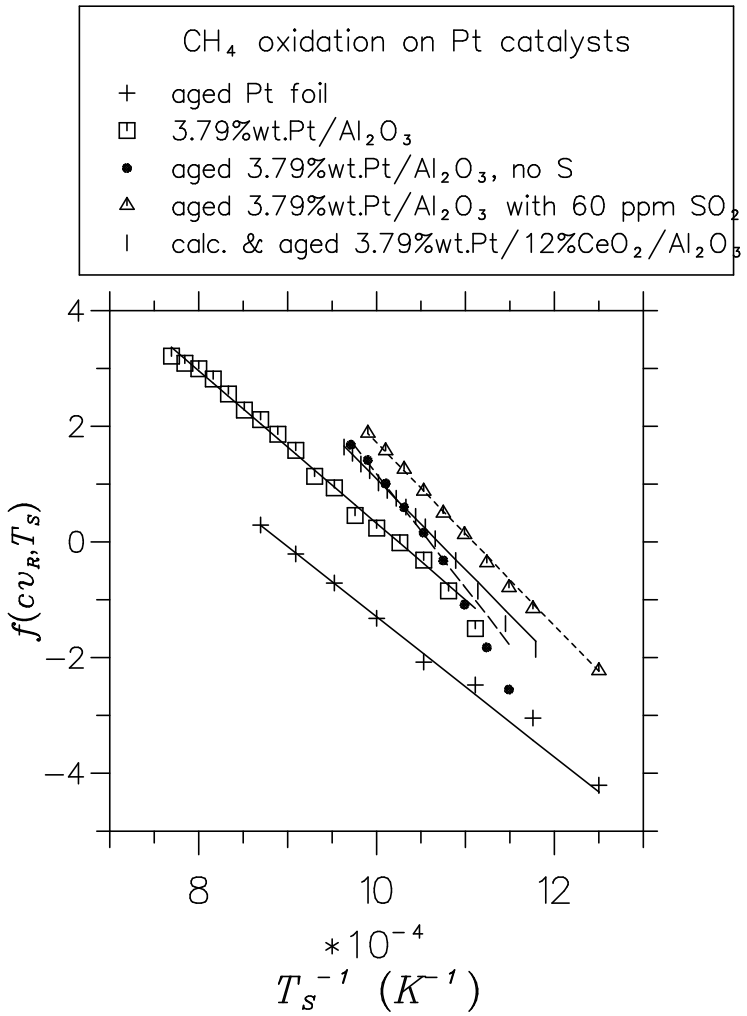

Fig. 2 Linear fits of *LHS* of Eq. 1 (called $f(cv_R,T_S)$) with T_S^{-1} for the lean oxidation of CH_4 in diluted air over various Pt catalysts, with and without S in the feed.

As the slope of each line is $-E/R$, shallow slopes indicate small activation energies. Intercepts with the ordinates axis yield the value of ln *A*, and as *A* is the frequency factor, it gives an

indication of the number of active sites on the catalyst. The projection of each line on the abcissae axis corresponds to the region of temperature of kinetic control for each experiment. When following a horizontal line in Fig. 2, one encounters from left to right the experiments for which decreasing catalyst temperatures yielded the same rate (i.e. catalysts of increasing activity). The values of *A* and *E* for each experiment are logged in Table 1. Note that with orders 0 in O_2 and 1 in CH_4, the unit of *A* is [cm s^{-1}], but that this unit can be converted to one more often encountered in applied catalysis kinetic studies by normalising *A* to the mass or molar quantity of the catalyst present on the foil. In this case, the foils had a 23.5 mm diameter, and the supported catalysts had densities of 0.82 and 0.52 mg of washcoat material per cm^2 of flat foil for Al_2O_3 and CeO_2/Al_2O_3 respectively.

Table 1. Arrhenius parameters used in the linear fits of Fig. 2. for the CH_4 lean oxidation on Pt catalysts, *A* is the frequency factor, *E* is the activation energy.

Fit	Catalyst	*A* (*cm* s^{-1})	*E* (kJ mol^{-1})
+	99.9% Pt foil	4.9×10^4	101
□	Pt/Al_2O_3	7.4×10^5	110
●	Aged Pt/Al_2O_3, no S	1.1×10^9	164
△	Aged Pt/Al_2O_3, 60 ppm SO_2	4.1×10^7	131
|	Calcined and Aged Pt / 12% Ce_2O_3 / Al_2O_3	1.8×10^7	130

Figure 2 and Table 1 attribute an apparent lower activity to the pure Pt foil compared to the washcoated foils. This is due to a lower number of active sites present for the same flat surface area of foil, as the porosity of the washcoats offers roughly one to two orders of magnitude more Pt sites than the pure Pt foil, reflected by the values of *A*. Figure 2 also shows that pure Pt or dispersed Pt on a washcoat exhibit similar activation energies if not exposed to the S-species, but that aging of the washcoated catalysts due to repeated use at high temperatures increases this value from 110 to 164 kJ/mol due to sintering of the Pt particles. This is in part counterbalanced by the effects of calcination of the washcoat upon first usage, opening and freeing previously blocked pores (increase in *A* from 7.5×10^5 to 1.1×10^9 cm s^{-1}).

The presence of trace SO_2 (and H_2S, not shown) on an aged washcoated catalyst slightly reduces the activation energy and increases the activity at any given temperature. This promoting effect

of sulphur species on the oxidation of hydrocarbons on precious metals seems contrary to the received wisdom that sulphur always acts as a catalyst poison, but has been encountered in previous studies only in the case of Pt /Al_2O_3 washcoats with propane oxidation [6] and methane oxidation [10]. The explanation given in [9] for this effect seems the most probable and involves the existence of occupied sites of O-$Pt^{(\delta+)}$ next to $(SO_4^{2-})^{(\delta-)}$-Al_2O_3 that are capable of withdrawing an electron away from the hydrocarbon reactant, activating its dissociation. This promoting effect could be counteracted by the 'poisoning' of a number of Pt sites by sulphates, as shown in a number of isothermal plug-flow micro-reactor studies [11-12]. Whether one effect outweighs the other in some experimental conditions would explain the contradictory findings of promotion and inhibition observed in different studies with similar Pt/Al_2O_3 catalysts. Fullerton *et al* [12] used the same Pt-washcoats in powder form with reactant flows of same composition as the present study in a plug-flow micro-reactor, and derived kinetics of the global reaction of lean oxidation of CH_4 using the conventional methodology. Using the densities of 1.13 g ml^{-1} and 1.16 g ml^{-1} for the Pt/Al_2O_3 and the Pt/CeO_2/Al_2O_3 washcoat powders respectively, the *A* values in the plug flow reactor study can be converted from ml s^{-1} g^{-1} to the unit used here, i.e. cm s^{-1}. A comparison of the Pt/Al_2O_3 catalyst kinetics (not exposed to S) yields a plug flow *A* value 150 times larger than that of the SPFR, and a slightly lower *E* (92 compared to 110 kJ mol^{-1}). Upon exposure to 30 ppm H_2S, the same catalyst in the plug flow reactor sees its *A* value double but *E* increase by 5 kJ mol^{-1}, resulting in slightly lower rates than prior to exposure. There is therefore in the plug flow experiments, a small inhibiting effect of H_2S on the CH_4 oxidation, as opposed to the SPFR which sees a promotion of the same reaction. By comparison, the plug flow rates are still two orders of magnitude larger than those of the SPFR upon exposure to H_2S. As the main difference between the two reactors kinetics is found in the value of *A*, one can venture that the number of active sites for a powder catalyst in plug flow conditions is far larger than that of the same catalyst fixed on a rigid surface as a washcoat. Whereas this sounds intuitively right, it is the extent of the discrepancy between the two types of kinetics which is surprising. This result has important implications for the modeller who utilises kinetics derived in plug-flow conditions from powder catalysts into reactor models simulating catalysts coatings, such as honeycomb monoliths or plate reactors. Our results show that doing so would greatly over-predict the activity of the catalyst when in the kinetic control regime. The fact that modelling results have been correct in the past in such situations could have been due to the flow conditions being in mass-transfer control.

4.2 Kinetics of CH_4 oxidation on Pd and Rh catalysts

Figure 3 shows results obtained for the lean oxidation of CH_4 in diluted air on the 2%wt.Rh/Al_2O_3 and 2%wt.Rh/12%CeO_2/Al_2O_3 washcoated foils in the presence and absence of small concentrations of H_2S in the feed. The corresponding kinetic parameters are then listed in Table 2.

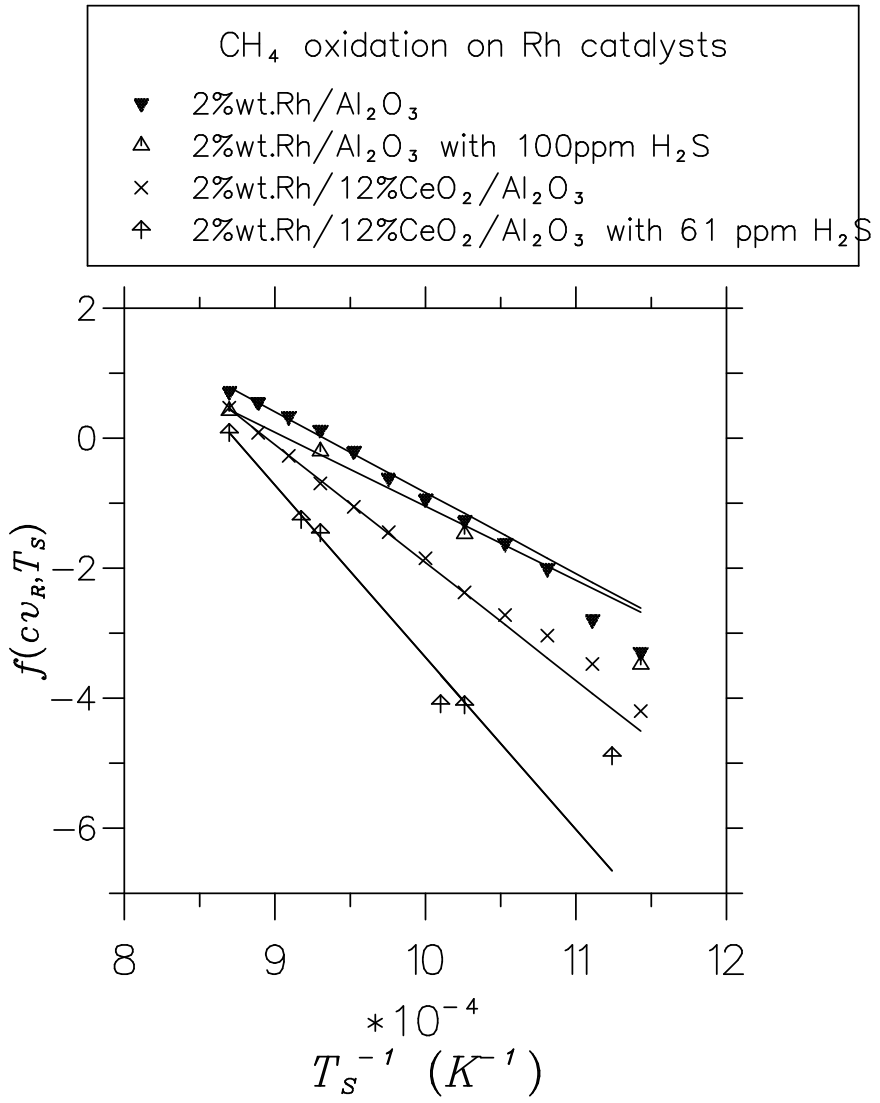

Fig. 3 Linear fits of *LHS* of Eq. 1 with T_S^{-1} for experiments of CH_4 lean oxidation on Rh catalysts.

Table 2. Arrhenius parameters used in the linear fits of Fig. 3 for the CH_4 lean oxidation on supported Rh catalysts in the presence and absence of H_2S in the feed.

Fit	Catalyst (all pre-calcined)	A ($cm\ s^{-1}$)	E (kJ mol^{-1})
▼	Rh/Al_2O_3	1.1×10^{5}	103
▵	Rh/Al_2O_3, 100ppm H_2S	3.1×10^{4}	95
×	Rh/12% Ce_2O_3 / Al_2O_3	1.1×10^{7}	151
⍋	Rh/12% Ce_2O_3 / Al_2O_3, 61ppm H_2S	1.1×10^{10}	220

The kinetic rates of the CH_4 oxidation on the Rh catalysts indicate that the Al_2O_3 and CeO_2/Al_2O_3 washcoats have different activities which are decreased by the presence of H_2S. The presence of ceria in the washcoat not only slows down the reaction but also makes the catalyst more sensitive to sulphur poisoning at low temperatures. In contrast, Rh/Al_2O_3 sees hardly any loss of activity from the presence of H_2S at low temperatures. In a study by Jones *et al* [11] using an isothermal plug flow micro-reactor and a similar catalyst exposed to a very-lean CH_4-air mixture doped with trace mercaptans (10 ppm), more severe poisoning effects were observed which reduced the rate by a ratio of 6. However, a regeneration treatment with H_2 flow brought back the rates to more than their original values. Nevertheless, as for the Pt catalyst, the kinetic rates obtained with Rh/Al_2O_3 powder catalyst in plug flow configuration were much faster than those derived here in the SPFR.

The results obtained on the 2.07%wt.Pd/Al_2O_3 and 2.07%wt.$Pd/12\%CeO_2/Al_2O_3$ washcoated foils in the presence and absence of small concentrations of H_2S are then shown in Fig. 4 and the corresponding Arrhenius parameters are summarised in Table 3.

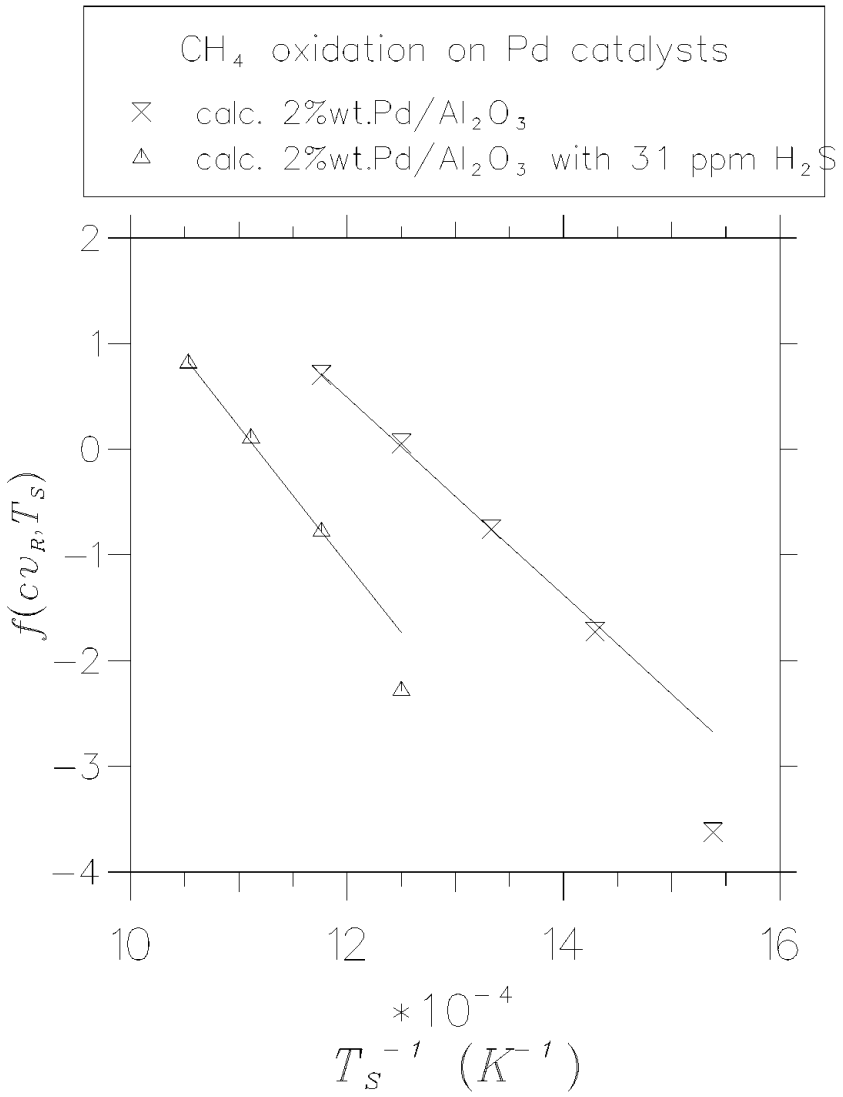

Fig. 4 Linear fits of *LHS* of Eq. 1 with T_S^{-1} for experiments of CH_4 lean oxidation on Pd catalysts, with and without H_2S in the feed.

Table 3. Arrhenius parameters used in the linear fits of Fig. 4 for the CH_4 lean oxidation on a supported Pd catalyst, in absence and presence of H_2S.

Fit	Catalyst (all pre-calcined)	*A* (*cm* s^{-1})	*E* kJ mol^{-1}
⧖	Pd/Al_2O_3	1.2×10^5	78
△	Pd/Al_2O_3, 31 ppm H_2S	1.9×10^6	108

The palladium catalyst studied here is clearly poisoned by the presence of H_2S in the feed. This result is in agreement with previous studies, as neutral or promoting effects due to S-species on the oxidation of hydrocarbons on Pd catalysts have, to the author's knowledge, not been reported to date. Figure 5 compares the activities of Pt, Rh, and Pd supported catalysts on Al_2O_3, in conditions where neither catalyst has yet been in the presence of sulphur species. Figure 5 shows the superiority of Pd to Pt and Rh in the lean oxidation of CH_4 at low temperatures, a well known behaviour, as shown previously by Burch and Loader [13].

Then Fig. 6 shows the same comparison when each of these catalysts is exposed to trace concentrations of sulphur species (H_2S or SO_2). These fits can also be found in the relevant figures 2-4 for the individual catalysts.

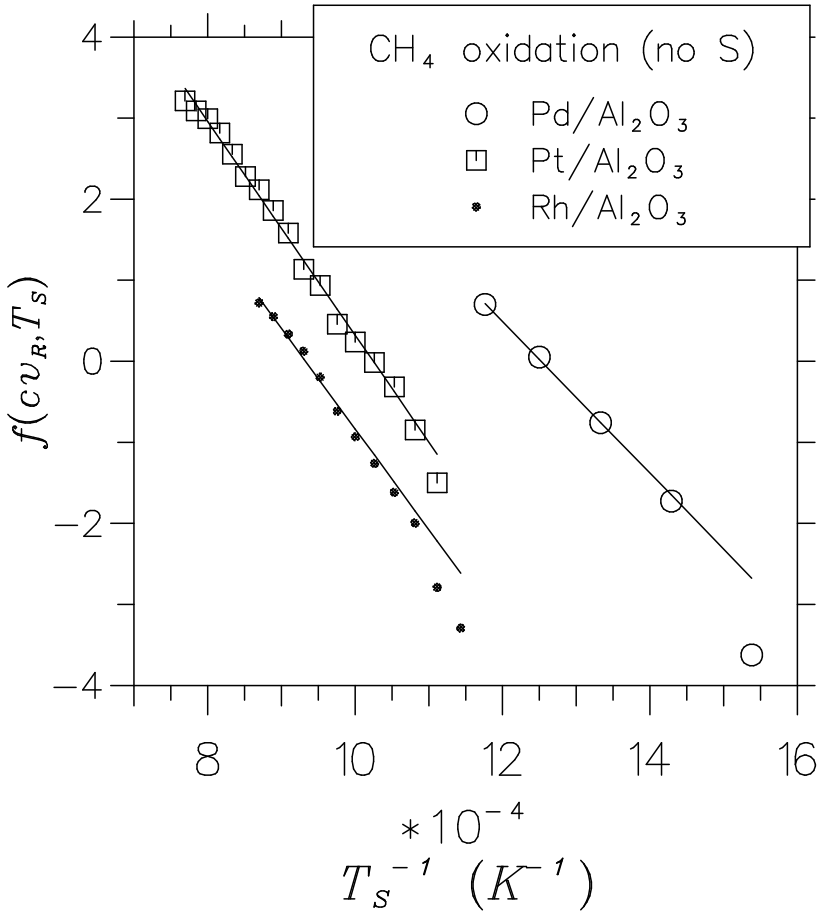

Fig. 5 Linear fits of the lean oxidation of CH_4 on Pd, Pt, and Rh supported on Al_2O_3, where neither catalyst has yet been exposed to sulphur-species.

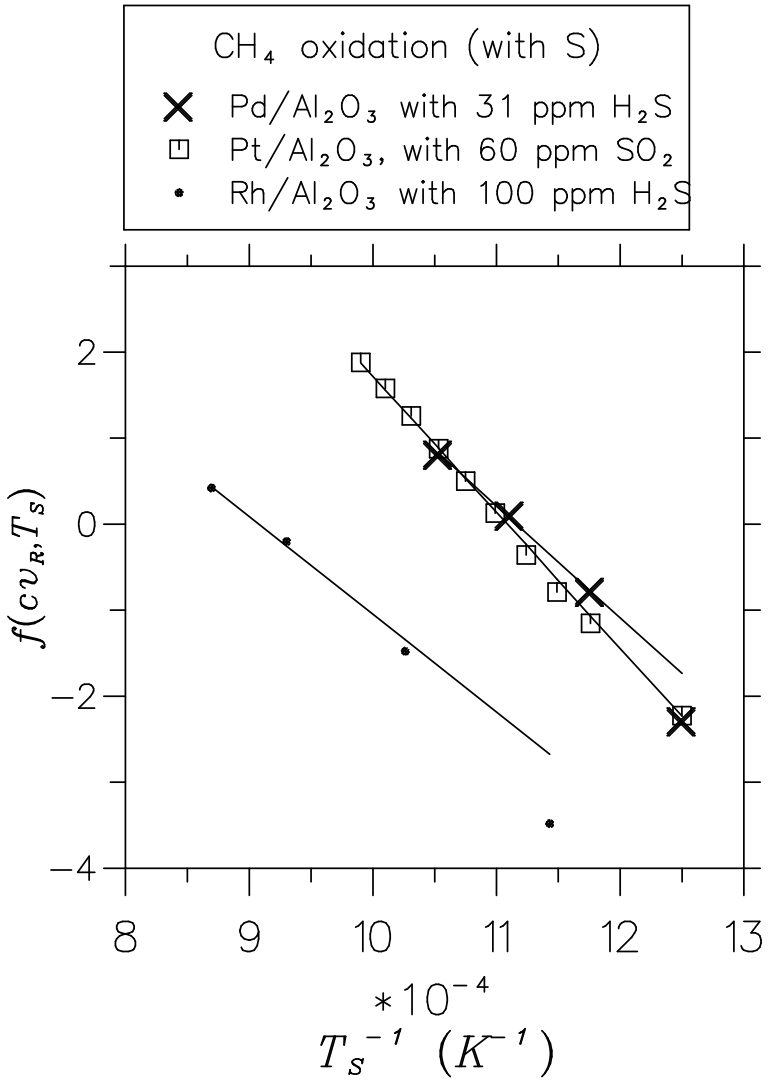

Fig. 6 As Fig. 5 but in presence of S in the feed.

Figure 6 shows how, upon exposure to S-species, the Pt and Pd catalysts exhibit comparable rates for lean CH_4 oxidation in the temperature range of the kinetically controlled regime. It is interesting to show that the conversion of CH_4 has a markedly different behaviour at higher temperatures for Pd than for Pt. Figure 7 plots the conversions of CH_4 on the Pt and Pd/Al_2O_3 catalysts exposed to the S-species for temperatures from ambient to 1200 K, following a cycle of increasing then decreasing temperature.

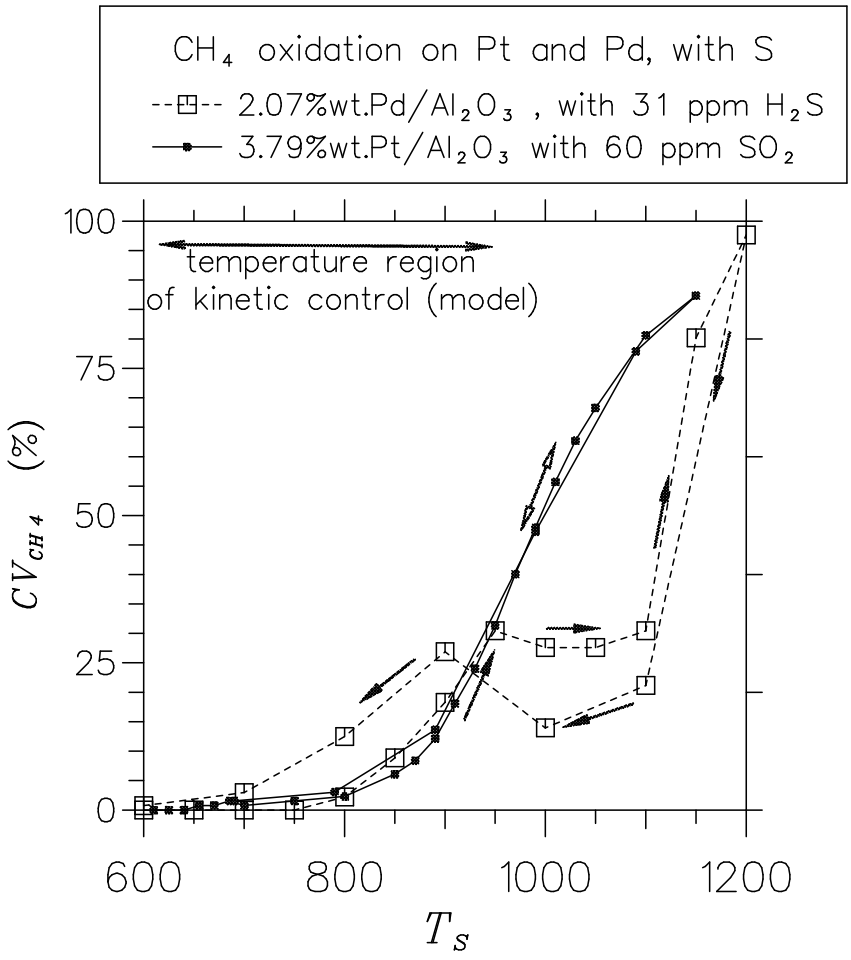

Fig. 7 Curves of CH_4 conversion (by oxidation to CO_2) *vs*. catalyst temperature on the Pt and on the Pd/Al_2O_3 catalysts in the presence of sulphur species in the feed. Arrows indicate whether the curves were obtained with a history of increasing or decreasing temperature.

The curves shown in Fig. 7 contrast the monotonic behaviour and lack of hysteresis exhibited by the Pt catalyst with that of Pd. The conversion curve of Pd with increasing temperature encounters a slight dip between 930 and 1100 K followed by a sharp increase in conversion up to 1200 K, which confers it a shape with characteristics seen in previous studies [14]. This is

attributed to the changing nature of the active site for CH_4 oxidation from PdO to Pd, less active. The sharp increase beyond 1100 K has not been determined with certainty to be due to either heterogeneous solid gas reactions or to gas phase ignition. One would expect that upon decreasing the temperature from 1200 K, the conversion would remain high if gas phase ignition had occurred. Instead, the conversion on the Pd catalyst follows the same curve back down to 1100 K, which would be consistent with an active heterogeneous site, probably metallic Pd. The activity of Al_2O_3 at high temperature has also often been invoked as a possible cause for this high temperature activity, but tests in the SPFR with the blank supports (Al_2O_3 and CeO_2/Al_2O_3 washcoated foils without precious metal) did not reveal a significant CH_4 conversion at 1100-1200 K. It is however possible that the coupled chemistries of Pd and Al_2O_3 cause an early heterogeneous CH_4 ignition on Al_2O_3. The observed hysteresis behaviour below 1100 K is also consistent with previous studies [15], and attributed to the Pd to PdO transformation. The active site for CH_4 oxidation on platinum catalysts, on the other hand, is universally agreed to be the Pt metal site, which explains the monotonic curve obtained.

If the promoting mechanism whereby interfacial sites of O-M next to (SO_4^{-2})-Al_2O_3 act as hydrocarbon dissociation promoter, where M = Pd, as was speculated earlier for M = Pt, then it is not surprising that sulphur in the feed does not induce an increase in the CH_4 oxidation rate on the Pd catalyst, as the O-Pd sites are competing on their own for the same reaction. The loss of surface area induced by the formation of metal sulphide clusters is then responsible for the observed decrease in conversion on the Pd catalyst in the presence of S-species, following a mechanism proposed in [11]. In [16], the authors explain the different effects of sulphating and non-sulphating supports on the inhibition of PdO activity catalysts by SO_2.

4.3 Kinetics of SO_2 and H_2S on blank and Pt catalysts

So far in this study, little distinction has been made between the effects of H_2S and SO_2 on the precious metal catalysts. This is due to the fact that the Al_2O_3 and the CeO_2/ Al_2O_3 washcoats are themselves active at low temperature in converting heterogeneously H_2S to SO_2, as shown in Fig. 8.

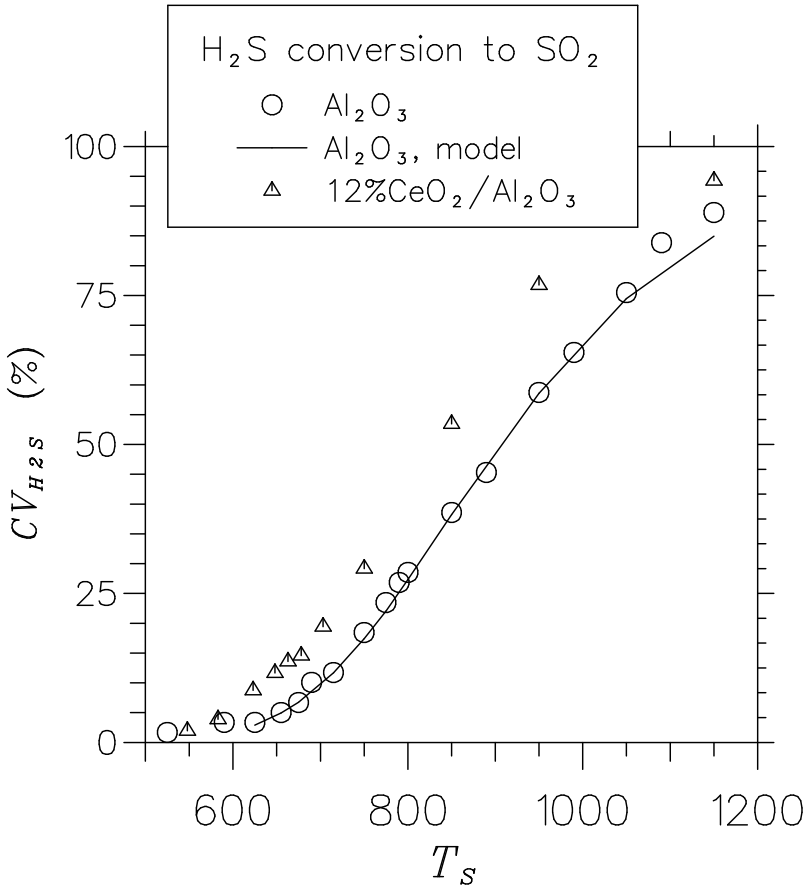

Fig. 8 Conversion of H_2S to SO_2 on the two blank supports when using 60 ppm of H_2S in a flow of air with an inlet velocity of 1.7 cm s^{-1}.

The kinetics derived on the basis of the global reaction $H_2S+1.5O_2 \rightarrow SO_2+H_2O$ on Al_2O_3 (order 0 in O_2 and 1 in H_2S) and the linear fits found for the (cv_{H2S}, T_S) data-pairs yielded $A = 5.8 \times 10^4$ cm s^{-1} and E = 68 kJ mol^{-1}, which produced the excellent agreement between model and experiments as shown in Fig. 8. Although this agreement is excellent all the way to 1100 K, the gas phase oxidation of H_2S to SO_2 in air is itself a process that does not require very high temperatures or long residence times, and we cannot ascertain that the conversion of H_2S to SO_2 observed above 750 K in Fig. 8 is not in fact, partly due to gas phase reactions. In addition, there is the possibility of formation of the secondary product SO_3, not detected by our analyser. Although we know from experiments in the SPFR that SO_2 does not convert to SO_3 in air on the blank supports, the presence of H-species when using H_2S might provide a route to SO_3 formation.

Thus when using trace H_2S and excess air on the precious metal supported catalysts, a large proportion of it would have converted to SO_2 prior or upon meeting with the catalyst, due to the sole activity of the washcoat material.

Moreover, further conversion of the H_2S to SO_2 and to SO_3 would have occurred from the activity of the precious metals themselves. For instance, we found that a 60 ppm SO_2/air flow on the Pt/Al_2O_3 catalyst exhibited a window of conversion to SO_3 in the temperature range 600-1150 K, with a peak at 900 K. The following rate parameters were derived for the reaction $SO_2+0.5O_2 \rightarrow SO_3$ (order 0 in O_2 and 1 in SO_2), on this catalyst in the kinetic control regime (600-750 K): $A = 2.2 \times 10^8$ cm s^{-1} and $E = 111$ kJ mol^{-1}. This window of conversion was unusual in that it showed higher temperatures than expected where SO_2 heterogeneous oxidation persists. According to the literature, sulphates, generally acknowledged as necessary intermediates in the heterogeneous oxidation of SO_2, remain stable up to 1033 K on Al_2O_3 [17], and up to 650 K on Pt [18].

5 Conclusions

The kinetics of the lean oxidation of CH_4 on Pt, Rh and Pd catalysts were derived using a new methodology that makes use of an experimental stagnation point flow reactor and its ideal numerical model. The rate data obtained showed that (i) the porous washcoats supported on steel foil were more active than the equivalent flat surface of pure precious metal (case of Pt), (ii) repeated use had activating (pore opening) then aging (sintering) effects, and (iii) Pd was more active than Pt, itself more active than Rh when not exposed to sulphur species and in the kinetic control regime, (iv) in general, the kinetic rates were much slower than equivalent rates measured for the same catalysts in powder form investigated in isothermal plug-flow conditions with the same mixture feeds.

Upon exposure to trace sulphur species H_2S and SO_2 in the gas feed, different behaviours were obtained for the three precious metals. The Pt catalysts exhibited a promotion of the CH_4 oxidation rate across the widest range of temperature (600-1200 K), the Pd/Al_2O_3 catalyst saw its rate significantly reduced, and that of the Rh/Al_2O_3 catalyst was slightly decreased. Similar effects have been found in the literature with respect to each of these findings. The ceria content of the Rh catalyst introduced more sensitivity to sulphur poisoning. The severe poisoning of the Pd catalyst meant that its activity in the kinetic control regime became comparable to that of the Pt catalyst in the same flow conditions.

The high temperature activity behaviour of Pt in presence of sulphur species in the feed was however superior to that of Pd, due to the changing nature of the active site in CH_4 oxidation (PdO/Pd), as is consistent with the literature based on other type of reactor studies.

Finally, it was found that although the blank catalysts were not active in oxidising SO_2 to SO_3 in air, they were able to convert efficiently H_2S to SO_2 at lower temperatures than those expected of gas phase chemistry. Thus, when using H_2S as a reactant in the presence of air on the catalysts studied, a significant fraction would have converted to SO_2 on the washcoat. A further fraction would have been converted by the precious metal, in particular Pt, which has been shown to be active in converting H_2S to both SO_2 and SO_3, the latter product persisting at temperatures unexpectedly high.

6 Acknowledgements

We thank the CVCP for an ORS award (S.-H. Zhang), and Johnson Matthey (Royston) for providing the catalysts.

7 References

1 Reinke, M., Mantzaras, J., Schaeren, R., Bombach, R., Inauen, A., Schenker, S., *combustion and Flame* 136 (2004) 217-240.

2 Lyubovsky, M., Pfefferle, L., *Catalysis Today* 47 (1999) 29-44

3 Joannon, M., Cavaliere, A., Faravelli, T., Ranzi, E., Sabia, P., Tregrossi, A., *Proceedings of the Combustion Institute* 30 (2005) 2605-2612.

4 Perger, T., Kovacs, T., Turanyi, T., Trevino, C., 2003. *J. Phys. Chem. B*, 107: 2262 (2003).

5 Aghalayam, P., Park, Y. K., Fernandes, N., Papavassiliou, V., Mahadeshwar, A.B., and Vlachos, D.G. *Journal of Catalysis*, 213:23 (2003).

6 Dupont, V., Zhang, S.-H., Jones, J.M., Rickett, G., and Twigg, M.V. Proceedings of the Seventh International Conference on Technologies and Combustion for a Clean Environment (Clean air 2003). 7-11, Lisbon, Portugal (2003).

7 Coltrin, M. E., Kee, R. J., Evans, G. H., Meeks, E., Rupley, F. M., & Grcar, J. F. SPIN (version 3.83). Sandia National Laboratories Report No. SAND91-8003.UC 401 (1991).

8 Dupont, V., Zhang, S. H., and Williams, A. *Chemical Engineering Science*, 56:2659 (2001).

9 Burch, R., Halpin, E., Hayes, M., Ruth, K, & Sullivan, J. A. *Applied Catalysis B:* Environmental, 19:199 (1998).

10 Lee, J. H., Trimm, D. L., & Cant, N. W. *Catalysis Today,* 47:353 (1999).

11 Jones, J. M., Dupont, V. A., Brydson, R., Fullerton, D. J., Nasri, N. S., Ross, A. B., & Westwood, A. V. K. *Catalysis Today*, 81(4):589 (2003).

12 Fullerton, D.J., Westwood, A. V. K., Brydson, R., Twigg, M. V., & Jones, J. M. (2003). *Catalysis Today*, 81(4):659 (2003).

13 Burch, R., & Loader, P. K. *Applied Catalysis B: Environmental* 5:149 (1994).

14 Euzen, P., Le Gal, J.-H., Rebours, B., and Martin, G. *Catalysis Today* 47:19 (1999).

15 Groppi, G., Cristiani, C., Lietti, L., Forzatti, P. Studies in Surface Science and Catalysis 130D:3801 (2000).

16 Lampert, J.K., Shahjahan Kazi, M., Farrauto, R.J. *Appl. Catal.* B 14:211 (1997).

17 Waqif, M., Pieplu, A., Saur, O., Lavalley, J. C., & Blanchard, G. *Solid State Ionics* 95:163 (1997).

18 Zebisch P., Stichler, M., Trischberger, P., Weinelt, M., & Steinruck, H.-P. *Surface Science*, 371:235 (1997).